Int J Heat Mass Transfer Vol 33, No 11, pp 2479–2489 1990
Printed in Great Britain

0017-9310/90 $3 00+0 00

Experimental and theoretical investigations on the steady-state and transient behaviour of a thermosyphon with throughflow in a figure-of-eight loop

P K VIJAYAN
Reactor Engineering Division, Bhabha Atomic Research Centre, Trombay, Bombay 400085 India

and

A. W DATE
Department of Mechanical Engineering, Indian Institute of Technology, Powai, Bombay 400076, India

(*Received April* 1989)

Abstract—This paper deals with experimental and theoretical investigations on a thermosyphon with throughflow in a figure-of-eight loop The one-dimensional energy and momentum conservation equations are solved with suitable assumptions and analytical solutions are obtained for the steady-state case for different throughflow inlet and outlet points The steady-state flow rates obtained with hot and cold leg injections are compared Comparison of predicted steady-state flow rates with experimental data shows agreement within ±15% The transient behaviour has been obtained numerically using the finite difference method and compared with experimental data

1. INTRODUCTION

IN THERMOSYPHON loops, the circulating fluid removes heat from a source and transports it to a sink, the fluid circulation being the result of the buoyancy force Thermosyphon loops find application in many fields, namely, gas turbine blade cooling, transformer cooling, nuclear reactor core cooling, solar heaters and geothermal processes A literature survey has revealed that thermosyphon studies have already been made in a number of loops of simple geometry The early studies by Welander [1] and Keller [2] were concerned with the stability of a thermosyphon in a loop with a point heat source and a point heat sink. Thereafter the toroidal loop has been the subject of extensive experimental and theoretical investigations probably due to its simplicity This is the only loop for which 1-D [3], 2-D [4] and 3-D [5] analyses have been reported. Experimental investigation of a thermosyphon in a toroidal loop has been carried out for the first time by Creveling *et al* [6] Later on, Damerell and Schoenhals [7] made an experimental investigation of the effect of the angular displacement of the heated and cooled sections of this loop. The double-loop toroidal thermosyphon was investigated by Sen *et al* [8]. Other loops studied include the parallel-channels loop of Chato [9], the square loop employed by Bau and Torrance [10], Hallinan and Viskanta [11], the rectangular loops of Lapin [12], Huang and Zelaya [13], the loops relevant to PWRs [14, 15] and the solar water heater [16]

There are very few thermosyphon studies in figure-of-eight loops. The loop employed in CANDU type pressurized heavy water reactors (PHWRs) has a figure-of-eight configuration Previous investigations of a thermosyphon in this loop have been carried out by Ardron *et al* [17] and Vijayan *et al* [18]

All the above studies have been carried out for closed loops without throughflow Throughflow effects are important for nuclear reactor cooling as some amount of feed and bleed is required even during thermosyphon conditions Zvirin [19] studied the effect of throughflow on a loop with two vertical branches with a point heat source and sink Mertol *et al* [20] studied the transient, steady-state and stability behaviour of a thermosyphon with throughflow in a toroidal loop. The temperature at which the throughflow enters the loop is also of practical relevance to nuclear reactor core cooling Some work is reported on this aspect by Zvirin [19] and Mertol *et al* [20] However, in all previous studies, the locations of the injection point and the bleed point were kept the same From the view point of nuclear reactor safety one is interested to know whether hot or cold leg injection is preferred which also has not been investigated previously. Further, all previous works on thermosyphons with throughflow were purely theoretical and no experiments with throughflow have been reported so far The present work, therefore, deals with experimental and theoretical investigations on a thermosyphon with throughflow.

NOMENCLATURE

A	cross-sectional area
A^*	parameter in equation (8), $A_e^2\gamma/V$
a, b	constants in equation (5)
C_p	specific heat
D	diameter
f	dimensional throughflow rate
F	non-dimensional throughflow rate
g	acceleration due to gravity
Gr_m	modified Grashof number, $D_e^3\rho^2\beta g\Delta T_r/\mu^2$
K	local loss coefficient
k	thermal conductivity
L	length
L_t	total circulation length
L_1	length of branch 1
L_2	length of branch 2
Nu'	Nusselt number, U_iZ_c/k
P	parameter in the definition of ψ', $4Nu'/(Re_s, Pr)$
Pr	Prandtl number, $C_p\mu/k$
Q	heat rate
Re	Reynolds number, $D_eW/A_e\mu$
S	non-dimensional coordinate around the loop
S_c	non-dimensional half length of the U-tube cooler
s	dimensional coordinate around the loop
t	time
T	temperature
ΔT_r	reference temperature difference used in the definition of Gr_m, $QZ_c/A_e\mu C_p$
U	overall heat transfer coefficient
V	volume
W	mass flow rate
Z	non-dimensional elevation
z	dimensional elevation
Z_1	elevation at cooler inlet
Z_2	elevation at header centre line
Z_c	centre line elevation difference between the cooler and the heater

Greek symbols

β	volumetric coefficient of expansion
γ	parameter in equation (3), $\int_0^{L_t} ds\, A(s)$
θ	non-dimensional temperature
μ	dynamic viscosity
ρ	density
τ	non-dimensional time
ϕ	parameter in equation (9), V_1/AZ_c
ψ'	parameter, $PS_c/(1+F)$
ω	non-dimensional flow rate

Subscripts

0	reference
c	cooler
e	equivalent
eff	effective
fi	throughflow inlet
fo	throughflow outlet
Ho	outside surface of heater tube
h	heater
I	integral
i	inside
l	loop
m	mean
s	secondary side of cooler
si	secondary inlet
ss	steady state.

2 THE EXPERIMENTAL INVESTIGATION

The experimental loop (see Fig 1) consisted of two horizontal heaters of annular geometry, with the inner tube directly heated by electric current. The heaters were connected to headers and the latter were connected to vertical inverted U-tube coolers by small diameter tubes Each cooler (tube-in-tube type) consisted of an inverted glass U-tube, the vertical portions of which were cooled by water flowing in the surrounding annulus formed with another glass tube The system pressure was maintained at near atmospheric by a small expansion tank provided at the highest elevation. The loop was insulated using precast asbestos magnesia

In the present loop all feed and bleed points are associated with the headers H1, H2, H3 and H4 as shown in Fig. 1 Injection is possible only in header 2, whereas the bleed flow could be taken out through any one of the four headers The inlet temperature of throughflow is the same as the inlet temperature of cooling water as the feed flow is branched off from the inlet side of the secondary cooling water line (see Fig. 1).

There were 24 thermocouples installed at various points in the loop (see Fig 1) to measure the heater surface and water temperatures All thermocouples were connected to a datalogger which could scan all the channels in less than 2 s The power input to the heater was obtained as the product of voltage and current which were measured The thermosyphon flow rate through the loop was then estimated from the measured heater power and temperature rise across the heater This method of flow measurement was compared against that measured by a magnetic flow meter under forced flow conditions and the agreement was found to be within 5–7% [21] The secondary side flow rates to the individual coolers were measured with the help of two rotameters The water temperatures at the inlet and outlet of both the coolers

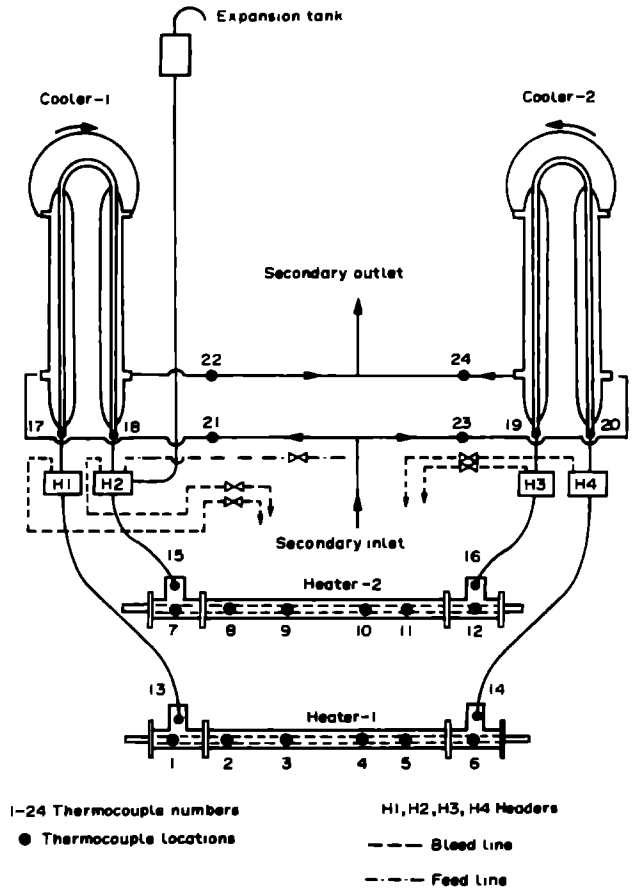

FIG 1 Experimental loop

were also measured. The throughflow rates were very small (<5 cm^3 s^{-1}) and were accurately measured by collecting the bleed flow in a measuring jar and noting the time

During the experiments the injection of water at room temperature was started after the system reached the steady-state thermosyphon condition with no throughflow A few seconds (about 5–6 s) later the bleed flow was started (this time delay does not have a significant effect on the transient behaviour as the transient is a slow one taking several minutes). Then the system was allowed to attain the new steady state with throughflow For fixed injection and bleed points hot or cold leg injection is obtained by changing the flow direction in the loop. During the transient, the loop temperatures were recorded at an interval of 1 min

3 METHOD OF ANALYSIS

The geometry and coordinate system considered for analysis is shown in Fig 2 The heaters are supplied with a constant power of Q_h and the coolers are supplied with a constant secondary mass flow rate of W_s at temperature T_{si} The loop is allowed to reach steady-state thermosyphon conditions At steady state a constant throughflow is suddenly introduced with inlet at header 2 and outlet at header 3. Thus for anticlockwise circulation, the flow rate in branch 1 (from header 2 to header 3 through heater 1) is higher than that in branch 2 (from header 3 to header 2 through heater 2) The assumptions made in the analysis are given below.

(1) The fluid properties are constant in the governing equations except for the body force term (Boussinesq approximation) where, the density variation with temperature is assumed linear, i.e. $\rho = \rho_0[1-\beta(T-T_0)]$.

(2) The effect of axial conduction and viscous dissipation in the fluid are neglected

(3) Perfect mixing is assumed to occur at the feed inlet

(4) The effective hydraulic resistance of each branch of the loop is assumed to be equal to the total loop resistance corresponding to the flow rate of the branch multiplied by the length fraction (L/L_t) of that branch

From the equation of continuity for one-dimen-

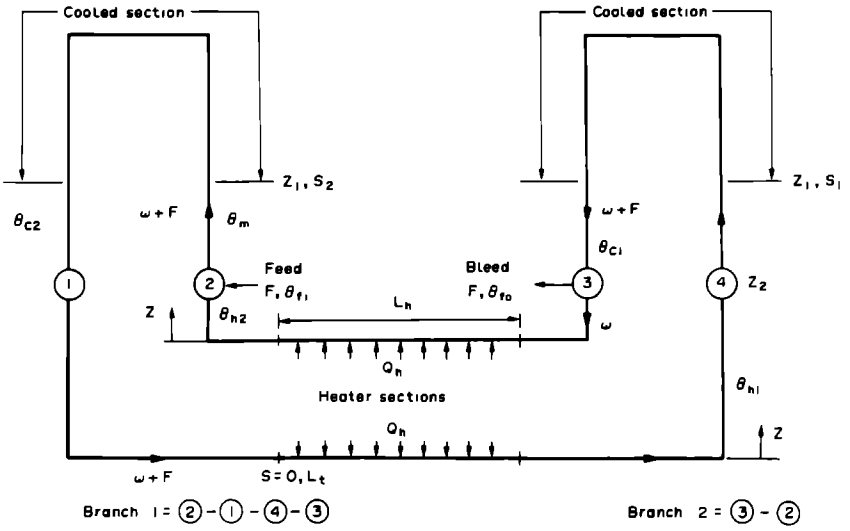

FIG 2 Loop considered for theoretical analysis

sional incompressible flow, we have that the mass flow rate in each branch of the loop is a function of time only Therefore, the momentum equation for the two branches can be written as follows

Branch 1

$$\gamma_1 \frac{d(W+f)}{dt} = g\beta\rho_0 \int_0^{L_1} T\,dz - K_1(W+f)^2/(2\rho_0 A_c^2) - (P_{hd3} - P_{hd2}) \quad (1)$$

Branch 2

$$\gamma_2 \frac{dW}{dt} = g\beta\rho_0 \int_0^{L_2} T\,dz - K_2 W^2/(2\rho_0 A_c^2) - (P_{hd2} - P_{hd3}) \quad (2)$$

where P_{hd2} and P_{hd3} are the pressures at header 2 and header 3, respectively Adding equations (1) and (2) yields

$$\gamma \frac{dW}{dt} = g\beta\rho_0 \int_0^{L_t} T\,dz - K_1(W+f)^2/(2\rho_0 A_c^2) - K_2 W^2/(2\rho_0 A_c^2) \quad (3)$$

The hydraulic loss coefficients K_1 and K_2 in equation (3) were obtained from

$$K_1 = K_{eff} L_1/L_t \quad \text{and} \quad K_2 = K_{eff} L_2/L_t \quad (4)$$

where K_{eff} is obtained from the following equation

$$K_{eff} = a/Re^b \quad (5)$$

where the constants a and b are obtained from the thermosyphon data generated in the present loop without throughflow The values of the constants a and b used in the analysis are 1.57×10^5 and 0.656, respectively [21] To solve equation (3) it is necessary to obtain the loop temperature distribution which can be obtained from the energy equation The energy equations for the two branches are

Branch 1

$$\frac{\partial T}{\partial t} + \left(\frac{W+f}{A\rho_0}\right)\frac{\partial T}{\partial s} = \begin{cases} 4qD_{Ho}/\{(D_i^2 - D_{Ho}^2)\rho_0 C_p\} & \text{heater 1} \\ -4U_i(T-T_s)/(D_i\rho_0 C_p) & \text{cooler} \\ 0 & \text{pipes} \end{cases} \quad (6a)$$

Branch 2

$$\frac{\partial T}{\partial t} + \left(\frac{W}{A\rho_0}\right)\frac{\partial T}{\partial s} = \begin{cases} 4qD_{Ho}/\{(D_i^2 - D_{Ho}^2)\rho_0 C_p\} & \text{heater 2} \\ 0 & \text{pipes} \end{cases} \quad (6b)$$

Note that branch 2 does not have any cooler The momentum and the energy equations are now non-dimensionalized using the steady-state parameters as described below

$$\omega = W/W_{ss}, \quad S = \frac{s}{Z_t}, \quad Z = \frac{z}{Z_t} \quad (7a)$$

$$\tau = t/t_{ch}, \quad \theta = (T - T_{ss})/(\Delta T_h)_{ss}, \quad F = f/W_{ss} \quad (7b)$$

where t_{ch} is the time required to pump one inventory of the loop through any cross-section at the steady-state condition. Hence

$$t_{ch} = V_t \rho_0 / W_{ss} \quad (7c)$$

The resulting dimensionless momentum equation is

$$A^* \frac{d\omega}{d\tau} + a[L_1(\omega+F)^{2-b} + L_2\omega^{2-b}]/(2Re_{ss}^b L_t) = (Gr_m/Re_{ss}^3)\int_0^{L_t} \theta \, dz \quad (8)$$

The dimensionless energy equations for the two branches are

Branch 1

$$\frac{\partial\theta}{\partial\tau} + \phi(\omega+F)\frac{\partial\theta}{\partial S} = \begin{cases} V_1/V_h & \text{heater} \\ -P\phi(\theta-\theta_s) & \text{cooler} \\ 0 & \text{pipes} \end{cases} \quad (9a)$$

Branch 2

$$\frac{\partial\theta}{\partial\tau} + \phi\omega\frac{\partial\theta}{\partial S} = \begin{cases} V_1/V_h & \text{heater} \\ 0 & \text{pipes} \end{cases} \quad (9b)$$

Energy balance at the injection point yields the following equation for the mixed mean temperature

$$\theta_m = (\omega\theta + F\theta_{fi})/(\omega+F) \quad (9c)$$

3 1 *Steady-state solutions*

The steady-state equations are obtained by dropping the $\partial/\partial\tau$ terms from equations (8) and (9) and setting $\omega = 1$ Exact analytical solutions of the steady-state equation can be obtained for specified Gr_m, θ_{si}, θ_{fi} and Nu_0 The steady-state temperature profile is obtained by integrating the steady-state energy equations for the two branches using the continuity of temperature as the boundary condition. The steady-state temperature profiles so obtained for the various segments (see Fig 2) of the loop are

$$\theta(S)_{ss} = \theta_{c2} + A_h Z_c S/[V_h(1+F)] \quad \text{heater 1} \quad (10a)$$

$$\theta_{ss} = \theta_{h1} = \theta_{c2} + 1/(1+F) \quad \text{hot leg 1} \quad (10b)$$

$$\theta(S)_{ss} = \theta_s + (\theta_{h1}-\theta_s)\exp\left(\frac{P}{1+F}\right)(S_1 - S) \quad \text{cooler 1} \quad (10c)$$

$$\theta_{ss} = \theta_{c1} = \theta_s + (\theta_{h1}-\theta_s)e^{-2\psi} \quad \text{cold leg 1} \quad (10d)$$

$$\theta(S)_{ss} = \theta_{c1} + A_h Z_c S/V_h \quad \text{heater 2} \quad (10e)$$

$$\theta_{ss} = \theta_{h2} = \theta_{c1} + 1 \quad \text{hot leg 2 until header 2} \quad (10f)$$

$$(\theta_m)_{ss} = (\theta_{h2} + F\theta_{fi})/(1+F) \quad \text{injection point} \quad (10g)$$

$$\theta_{ss} = (\theta_m)_{ss} \quad \text{hot leg 2 until cooler 2} \quad (10h)$$

$$\theta(S)_{ss} = \theta_s + (\theta_m - \theta_s)\exp\left(\frac{P}{1+F}\right)(S_2 - S) \quad \text{cooler 2} \quad (10i)$$

$$\theta_{ss} = \theta_{c2} = \theta_s + (\theta_m - \theta_s)e^{-2\psi} \quad \text{cold leg 2} \quad (10j)$$

Using equation (10) the integral in the momentum equation (8) can be evaluated as

$$\theta_1 = \int_0^{L_t} \theta \, dZ = Z_1[\theta_{h1} + \theta_m - \theta_{c1} - \theta_{c2}] + Z_2(\theta_{h2} - \theta_m) + (\theta_{h1} + \theta_m - 2\theta_s)\left(\frac{1+F}{P}\right)[1 + e^{-2\psi} - 2e^{-\psi}]$$

Substituting this in equation (8), the steady-state Reynolds number with throughflow can be obtained as

$$Re_{ss} = [2Gr_m\theta_1 L_t/\{a(L_1(1+F)^{2-b} + L_2)\}]^{1/(3-b)} \quad (11)$$

3.1 1 *Steady-state solutions for other feed and bleed points.* It may be noted that equations (10) and (11) apply only for injection in header 2 and bleed from header 3 and the anticlockwise flow direction shown in Fig. 2 If the flow direction or the location of injection and bleed points are different from that in Fig 2, then the solutions are also different. Following the same methodology described above, the steady-state equations similar to equations (10) and (11) were derived for other feed and bleed locations. These solutions are presented in ref. [21] for the anticlockwise and clockwise flow directions, respectively, but are not reproduced here due to shortage of space

3 2 *Transient solution*

Transient analysis of a thermosyphon loop is usually done numerically employing the finite difference method Analytical methods for the transient behaviour on the other hand are mainly concerned with the evaluation of the characteristic time constant of the system of Zvirin *et al* [15]. In some restricted cases, analytical methods can also be employed to obtain an approximate transient behaviour as discussed by Zvirin [22]. The coupled, time-dependent governing equations (8) and (9) have been solved numerically by using the finite difference method The energy equations were advanced explicitly using the backward difference formula for the spatial derivatives and the forward difference formula for the time derivatives The time step was chosen so as to satisfy the stability criteria. The momentum equation was solved implicitly using the Newton–Raphson method The integral in the momentum equation was evaluated using Simpson's rule Details of the numerical solution and

the discretization scheme employed are given in ref [21]

3 3 *Efficiency of throughflow*

The throughflow efficiency η, is defined as the ratio of the energy carried away by the throughflow to the total energy added to the loop At steady-state conditions this is given by

$$\eta_{ss} = fC_p(T_{fo} - T_{fi})/2Q_h \tag{12}$$

or

$$\eta_{ss} = \frac{F}{2}(\theta_{fo} - \theta_{fi}) \tag{13}$$

For the transient condition the instantaneous efficiency is given by

$$\eta(\tau) = \frac{F}{2}\{\theta_{fo}(\tau) - \theta_{fi}\} \tag{14}$$

4. MANNER OF PRESENTATION

From equations (8) and (9) it is clear that the performance of the present loop under throughflow conditions is governed by the parameters F, θ_{fi}, location of feed and bleed and flow direction in addition to Gr_m, Nu_0 and θ_{si} Effect of variation of Gr_m, Nu_0, θ_{fi} and θ_{si} on the thermosyphon behaviour is outside the scope of the present investigation Since injection was possible only in header 2 in the present loop, the following equation can be written

$$Re(\tau) = f(F, \text{bleed location and flow direction}) \tag{15}$$

The effect of all the parameters given by equation (15) are investigated for the steady-state case where analytical solutions exist

For the transient case, however, the equations are to be solved numerically and hence injection in header 2 and bleed from header 3 only is considered. Also, for the transient case, only one flow direction is considered (anticlockwise direction given in Fig. 2) For this flow direction and feed and bleed arrangement the effect of F on the transient behaviour is studied

In the present study, the initial condition considered is one of steady-state thermosyphon at the specified Gr_m and secondary conditions without throughflow The initial temperatures and flow rates were estimated using equations (10) and (11) with $F = 0$

5 DISCUSSION OF RESULTS—STEADY-STATE SOLUTION

5 1 *Re_{ss} vs F—comparison with experiment*

In Fig 3 the effect of F on the predicted Re_{ss} for throughflow entering header 2 and leaving header 3 is presented for both flow directions In this case the anticlockwise direction is seen to give a lower flow than the clockwise direction The effect of throughflow is to reduce the thermosyphon flow rate when compared to that obtained without throughflow The measured flow rates are also plotted in this figure The predicted Reynolds numbers are seen to fall within $\pm 15\%$ of data

5.2 *Effect of bleed point location*

From Fig 4 it is seen that for a fixed injection point the thermosyphon flow rate also depends on the location of the bleed point For injection in header 2, the best flow rate is obtained for bleeding from header 2. The next best flow rate is obtained for bleeding from header 1, followed by header 4 and header 3 In other words the best flow rate is obtained for minimum distance in the direction of flow between the points of injection and bleed This is to be expected as the effect of throughflow is to reduce the buoyancy force and to increase the frictional resistance

As the throughflow rate increases, the efficiency of throughflow increases Bleeding from hot legs leads to significantly higher efficiency than bleeding from cold legs Though, the best efficiency of throughflow is obtained for bleeding from header 4, it leads to very low mass flow rates in one of the heaters and consequently high heater temperatures

5.3. *Hot leg injection vs cold leg injection (effect of flow direction)*

From the above results it has been established that the thermosyphon flow rate depends on the distance between the points of injection and bleed Hence to study whether hot leg or cold leg injection is preferred one has to locate the feed and bleed points in such a way that both the branches of the loop (the low flow branch and the high flow branch) are of equal lengths irrespective of flow direction This condition is satisfied for injection in header 2 and bleeding from header 4 The results of this study are given in Fig 5 From this figure it is seen that with hot leg injection the flow rate is only marginally lower than that obtained with cold leg injection This is because in a figure-of-eight configuration each half of the loop contributes to the buoyancy driving force and the reduction in buoyancy force due to hot leg injection in one half of the loop is partially compensated by the accompanying increase in the contribution to the buoyancy force in the other half of the loop The increase in buoyancy force, however, is obtained only by a corresponding increase in the heater surface temperature in the low flow branch The available experimental data are also plotted in Fig 5 which show good agreement with the predictions

Figure 6 shows a case (injection in header 2 and bleed from header 1) where the hot leg injection leads to larger thermosyphon flow rates than the cold leg injection Here the reduction in the thermosyphon flow rate due to hot leg injection is more than compensated by the length effect It may be noted that throughflow travels only a short length inside the loop with hot leg injection, while with cold leg injection it travels a

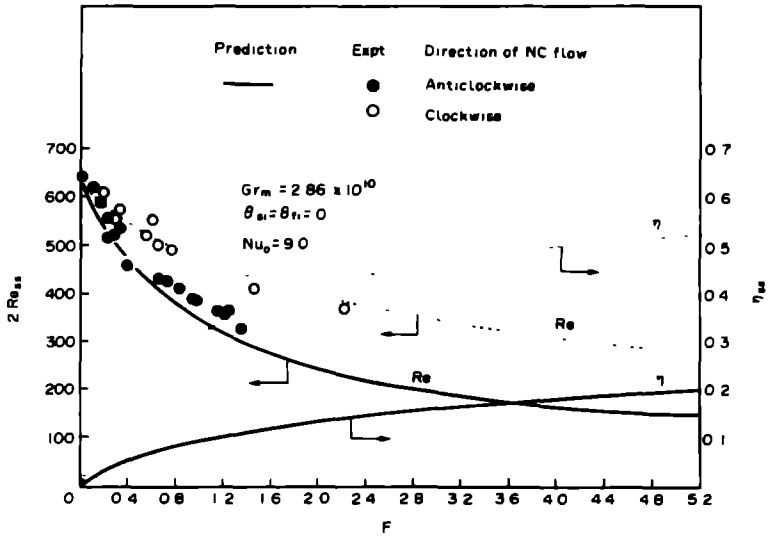

FIG 3 Comparison of measured and predicted flows (injection in header 2 and bleeding from header 3)

longer length and that is the reason for getting larger flows with hot leg injection However, the larger flow is obtained at the cost of an increased fluid temperature in the low flow branch

5.4. *Typical loop temperature distribution*

Typical non-dimensional loop temperature distribution for different throughflow rates are shown in Fig 7 When the throughflow rate is zero, we get a symmetric temperature distribution in each half of the loop With a throughflow, the temperature distribution becomes asymmetric due to the unequal flows in the different branches of the loop With the increase in throughflow, this asymmetry in temperature distribution keeps growing

6. DISCUSSION OF RESULTS—TRANSIENT SOLUTION

The transient solutions presented in this paper are for small throughflow rates (i.e $F < 1$) as instability is observed for large throughflows

6.1 *Comparison with experiment (feed in header 2–bleed from header 3)*

Figure 8 shows the predicted and measured transient behaviour of $\Delta\theta_{h1}$ and $\Delta\theta_{h2}$ at $Gr_m = 2.67 \times 10^{10}$ and $F = 0.7009$ It is seen from this figure that the trends observed in the experiments are predicted correctly except for a small period during the initial stage The initial dip seen in the experimental curve of $\Delta\theta_{h2}$

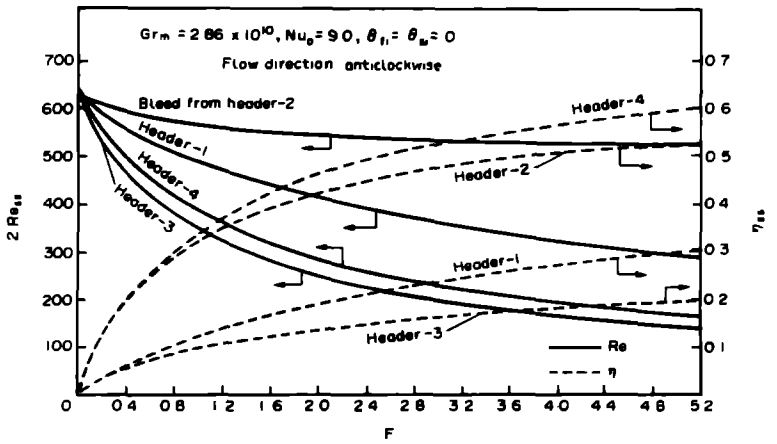

FIG 4 Effect of bleed point location on natural circulation flow (injection in header 2)

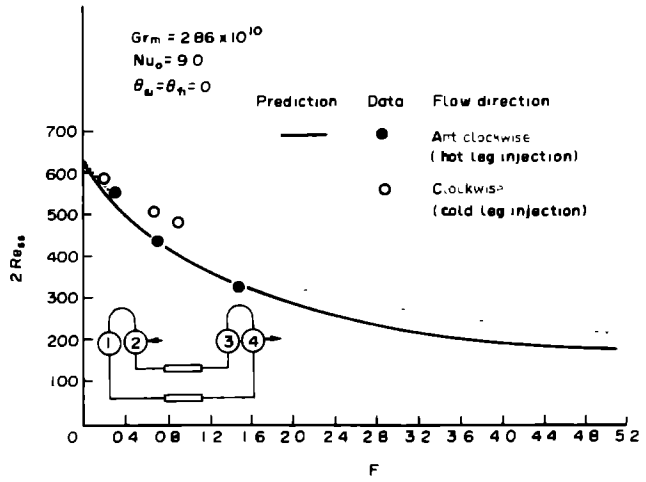

FIG 5 Effect of flow direction (steady state)

is due to the occurrence of a small backflow at the time of opening the bleed valve In the calculations, this backflow is not accounted for Though, the experimental curve shows oscillatory behaviour, there are too many oscillations in the predicted curve This is expected as the numerical model employed does not consider the effect of the secondary flows and the thermal lag of the walls of the loop and the heater

6.2 *Effect of small throughflow* ($F < 1\ 0$)

Figure 9 shows the predicted efficiency variation as a function of throughflow For low throughflow rates ($F = 0\ 1$) the η jumps to the steady-state value quickly and remains steady As the throughflow rate increases ($F = 0\ 25$) small oscillations in η with time appear With further increase in throughflow, the amplitude and frequency of these oscillations increase ($F = 0\ 5$ and $1\ 0$) The time required to attain the steady-state value also increases with F

Figure 10 shows the predicted transient flow rate in branch 2 for different throughflow rates For low throughflow rates the thermosyphon flow experiences some initial oscillations before reaching the steady state The steady-state flow rate, however, is lower when compared to the case without throughflow (i e. $F = 0$). As the throughflow rate increases the amplitude and frequency of these initial oscillations increase

7. CONCLUSIONS

Throughflow tends to reduce the thermosyphon flow rate when compared to the case without throughflow. As the throughflow rate increases, the thermosyphon flow rate decreases while the efficiency increases For a given injection point, the steady thermosyphon flow rate depends on the location of the bleed point Best flow rates are obtained for minimum distance in the direction of flow between the injection and bleed points. Hot leg injection does not always give

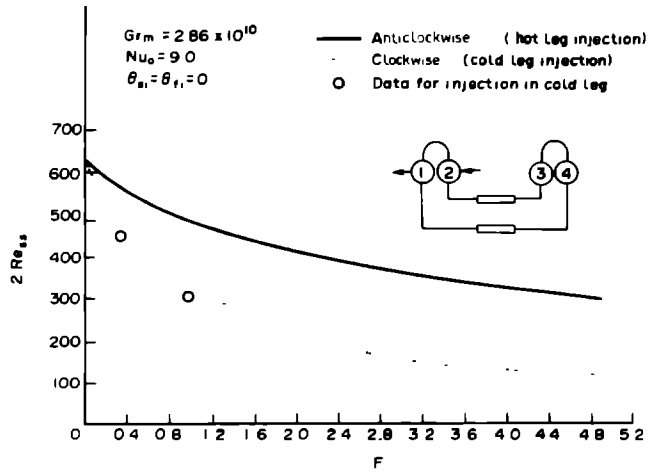

FIG 6 Effect of flow direction (steady state)

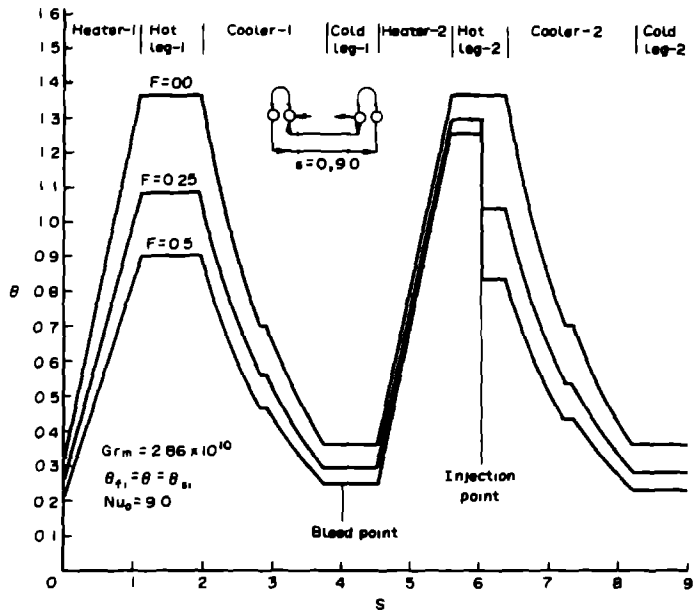

FIG 7 Effect of throughflow on steady-state temperature distribution.

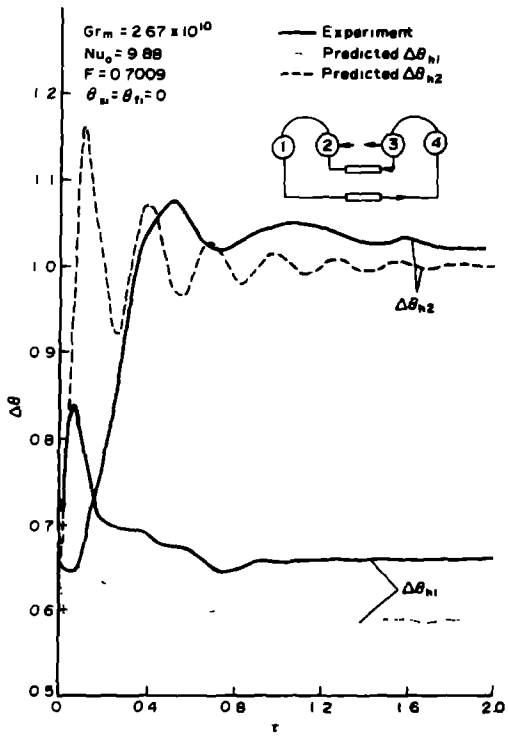

FIG 8 Predicted and measured transient with throughflow.

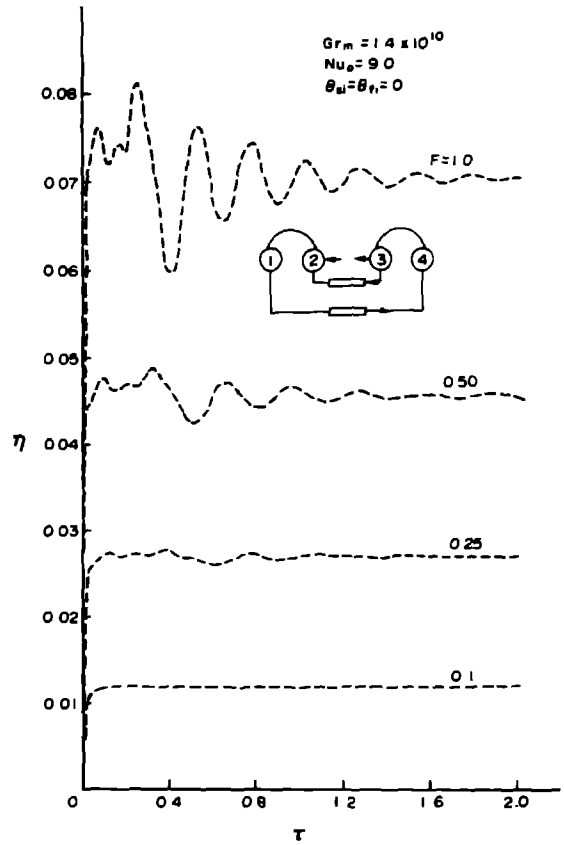

FIG 9 Effect of throughflow on η (transient state)

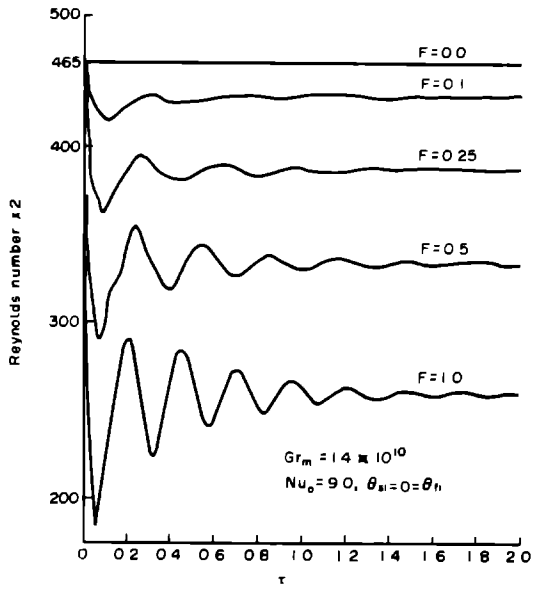

FIG 10 Effect of throughflow on the transient performance of a thermosyphon

lower flow rate compared to cold leg injection With a throughflow, the loop temperature distribution becomes asymmetric and this asymmetry keeps growing with increase in throughflow rate Measured values of steady flows are found to be within ±15% of the predictions

Predicted transients with $F \leqslant 1$ show initial oscillations of increasing amplitude and frequency before reaching steady state as the throughflow rate is increased Comparison of predicted and measured transients shows that the trends observed in experiments are correctly predicted

Acknowledgements—The authors wish to express their gratitude to Mr S K Mehta (Director, Reactor Group, BARC) for his support and encouragement in carrying out this work.

REFERENCES

1 P Welander, On the oscillatory instability of a differentially heated loop, *J Fluid Mech* **29**, 17–30 (1967).
2 J B Keller, Periodic oscillations in a model of thermal convection, *J Fluid Mech* **26**, 599–606 (1966)
3 R Greif, Y Zvirin and A Mertol, The transient and stability behaviour of a natural circulation loop, *J Heat Transfer* **101**, 684–688 (1979)
4 A Mertol, R Greif and Y Zvirin, Two-dimensional study of heat transfer and fluid flow in a natural convection loop, *J Heat Transfer* **104**, 508–514 (1982)
5 A S Lavine, R Greif and J A C Humphrey, A three dimensional analysis of natural convection in a toroidal loop—the effect of Grashof number, *Int J Heat Mass Transfer* **30**, 251–261 (1987)
6 H F Creveling, J F De Paz, J Y Baladi and R J Schoenhals, Stability characteristics of a single-phase free convection loop, *J Fluid Mech* **67**, 65–84 (1975)
7 P S Damerell and R J Schoenhals, Flow in a toroidal thermosyphon with angular displacement of heated and cooled sections, *J Heat Transfer* **101**, 672–676 (1979)
8 M Sen, D A Pruzan and K E Torrance, Analytical and experimental study of steady-state convection in a double-loop thermosyphon, *Int J Heat Mass Transfer* **31**, 709–722 (1988)
9 J C Chato, Natural convection flows in parallel-channel systems, *J Heat Transfer* **85**, 339–345 (1963)
10 H H Bau and K E Torrance, Transient and steady behaviour of an open, symmetrically heated, free convection loop, *Int J Heat Mass Transfer* **24**, 597–609 (1981)
11 K P Hallinan and R Viskanta, Heat transfer from a vertical tube bundle under natural circulation conditions, *Int J Heat Fluid Flow* **6**, 256–264 (1985)
12 Y D Lapin, Heat transfer in communicating channels under conditions of free convection, *Thermal Engng* **16**, 94–97 (1969)
13 R J Huang and R Zelaya, Heat transfer behaviour of a rectangular thermosyphon loop, *J Heat Transfer* **110**, 487–493 (1988)
14 G G Loomis and K Soda, Results of the semi scale MOD-2A natural circulation experiments, NUREG/CR-2335 and EGG-2200, Idaho National Engineering Laboratory (1982)
15 Y Zvirin, P R Jeuck III, C W Sullivan and R B Duffey, Experimental and analytical investigation of a natural circulation system with parallel loops, *J Heat Transfer* **103**, 645–652 (1981)
16 K S Ong, A finite-difference method to evaluate the thermal performance of a solar water heater, *Solar Energy* **16**, 137–147 (1974)
17 K H Ardron, V S Krishnan, G R McGee, J W D Anderson and E H Hawley, Two-phase natural circulation experiments in a pressurised water loop with figure-of-eight symmetry, *Experimental and Modelling Aspects of Small-break LOCA, Proc Specialists' Meeting*, IAEA, Budapest, Hungary, 3–7 October (1983)
18 P K Vijayan, V Venkat Raj, S K Mehta and A W Date, Phenomenological investigations in a loop relevant to a PHWR, ASME WAM Paper No 85-WA/HT-17 (1985)
19 Y Zvirin, The effects of a throughflow on the steady state and stability of a natural circulation loop, *Proc 19th Natn Heat Transfer Conf*, Orlando, Florida (July 1980)
20 A Mertol, R Greif and Y Zvirin, The transient, steady state and stability behaviour of a thermosyphon with throughflow, *Int J Heat Mass Transfer* **24**, 621–633 (1981)
21 P K Vijayan, Investigations on the single-phase thermosyphon in a figure-of-eight loop relevant to pressurised heavy water reactors, Ph D Thesis, Indian Institute of Technology, Bombay (1988)
22 Y Zvirin and R Greif, Transient behaviour of natural circulation loops two vertical branches with point heat source and sink, *Int J Heat Mass Transfer* **22**, 499–504 (1979)

ETUDES EXPERIMENTALES ET THEORIQUES DU COMPORTEMENT D'ETATS PERMANENT ET TRANSITOIRE D'UN THERMOSIPHON AVEC BOUCLE EN FORME DE HUIT

Résumé—On décrit les recherches expérimentales et théoriques sur un thermosiphon avec boucle en forme de huit. Les équations monodimensionnelles d'énergie et de quantité de mouvement sont résolues à partir d'hypothèses convenables et des solutions analytiques sont obtenues dans le cas permanent pour différents points d'entrée et de sortie. Les débits permanents obtenus, avec des injections dans la branche chaude ou froide, sont comparés aux données expérimentales. La comparaison entre débits calculés et débits mesurés montre un accord à mieux que ± 15%. Le comportement variable a été obtenu numériquement en utilisant une méthode de différences finies et on a comparé avec l'expérience.

EXPERIMENTELLE UND THEORETISCHE UNTERSUCHUNG DES STATIONÄREN UND INSTATIONÄREN VERHALTENS EINES THERMOSYPHONS IN DOPPELSCHLEIFENANORDNUNG

Zusammenfassung—Es wird über experimentelle und theoretische Untersuchungen an einem Thermosyphon in Doppelschleifenanordnung berichtet. Die eindimensionalen Erhaltungsgleichungen für Energie und Impuls werden bei geeigneten Annahmen gelöst. Es ergeben sich analytische Ausdrücke für den stationären Fall bei Wahl unterschiedlicher Eintritts- und Austrittspunkte der Durchströmung. Für stationäre Strömungsbedingungen werden die Fälle miteinander verglichen, bei denen der Austrittspunkt einmal im heißen und einmal im kalten Teil liegt. Ein Vergleich der berechneten Ergebnisse mit Versuchsdaten zeigt eine Übereinstimmung innerhalb ± 15%. Zusätzlich wird mit Hilfe eines Finite-Differenzen-Verfahrens das Übergangsverhalten berechnet und ebenfalls mit Versuchsdaten verglichen.

ЭКСПЕРИМЕНТАЛЬНОЕ И ТЕОРЕТИЧЕСКОЕ ИССЛЕДОВАНИЕ СТАЦИОНАРНОГО И НЕСТАЦИОНАРНОГО ПОВЕДЕНИЯ ТЕРМОСИФОНА СО СКОВОЗНЫМ ПОТОКОМ В КОНТУРЕ В ФОРМЕ ВОСЬМЕРКИ

Аннотация—Экспериментально и теоретически исследуется термосифон со сквозным потоком в контуре в форме восьмерки. При соответствующих допущениях решаются одномерные уравнения сохранения энергии и импульса, и определяются аналитические решения для стационарного случая и различных точек входа и выхода сквозного потока. Сравниваются значения стационарных расходов при подаче холодной и горячей сред. Сравнение показало, что рассчитанные и экспериментальные данные совпадают с точностью ± 15%. Методом конечных разностей рассчитано нестационарное поведение, и проведено сравнение полученных результатов с экспериментальными данными.